

Initial formation of estuarine sections

H.M. Schuttelaars¹, H.E. de Swart¹ and G.P. Schramkowski¹

Abstract: A simple model is developed to describe the initial evolution of bedforms in tidal embayments. The water motion is modelled by the depth-integrated shallow water equations. The system is forced by a prescribed free surface elevation at the entrance of the embayment. The sediment is transported both due to advective and diffusive processes. Tidal averaging is used to obtain the bottom profiles at the long morphological time scale.

It is shown that an equilibrium bed without a lateral structure is unstable with respect to perturbations with a lateral structure. Two types of perturbations with different length scales are encountered: one type of instability scales with the length of the embayment and is mainly driven by convergences and divergences of diffusive fluxes, whereas the other type has much shorter wavelengths. The latter type is maintained due to convergences and divergences of advective sediment fluxes. The physical processes involved depend on tidal and geometrical characteristics. It is proposed that some of the large-scale features in tidal embayments, such as estuarine sections, might be related to the instabilities that scale with the embayment length.

1 Introduction

In estuaries very energetic conditions are encountered which may result in modifications of the bathymetry and the characteristics of sediment distribution on spatial and time scales ranging from a few seconds and centimeters to centuries and hundreds of kilometers [9]. Because of the strong tidal currents in the channels and the lower parts of the flanking tidal flats, sediment can be transported and undulations can develop. Field data indicate that different types of bed forms can exist. On the one hand, near the entrance of shallow embayments (e.g. those located along the east coast of the United States) so-called estuarine bars are often observed [3]). These rhythmic bars have wave-lengths which scale with the width of the embayment and do not migrate. On the other hand deeper embayments, e.g. those located in the Dutch and German Wadden Sea, are characterised by a fractal pattern of channels [c.f. 5, 1] which appear to scale with the length of the embayments if the embayment length is short compared to the tidal wave-length. In many embayments both types of bottom patterns can be observed simultaneously. An example is the Western Scheldt, a tidal embayment located at the Dutch-Belgium border (see figure 1). Its length from Vlissingen up to Gent is about 160 km. The width of the estuary decreases from approximately 6 km at the mouth to less than 100 m near Gent, while its depth decreases from approximately 15 m to only 3 m at the landside. The estuary can be divided in three parts, a sub-tidal delta west of Vlissingen, a multiple channel system separated by elongated shoals in the seaward marine part between Vlissingen and Doel and a single tidal channel landward of Doel. In this contribution we will be mainly concerned with the seaward marine section. This section can be subdivided in six distinct estuarine sections (see figure 2). Each estuarine section has a large meander-shaped main ebb channel and a laterally bordering large straight main flood channel. These channels are usually separated by shoals and linked by connecting channels. Within these sections, bars are observed. The system is mainly driven by tidal currents, the mean river outflow is less than one percent of the tidal volume [16, 6].

¹Institute for Marine and Atmospheric Research, Utrecht University, P.O.Box 80.005, 3508 TA Utrecht, The Netherlands

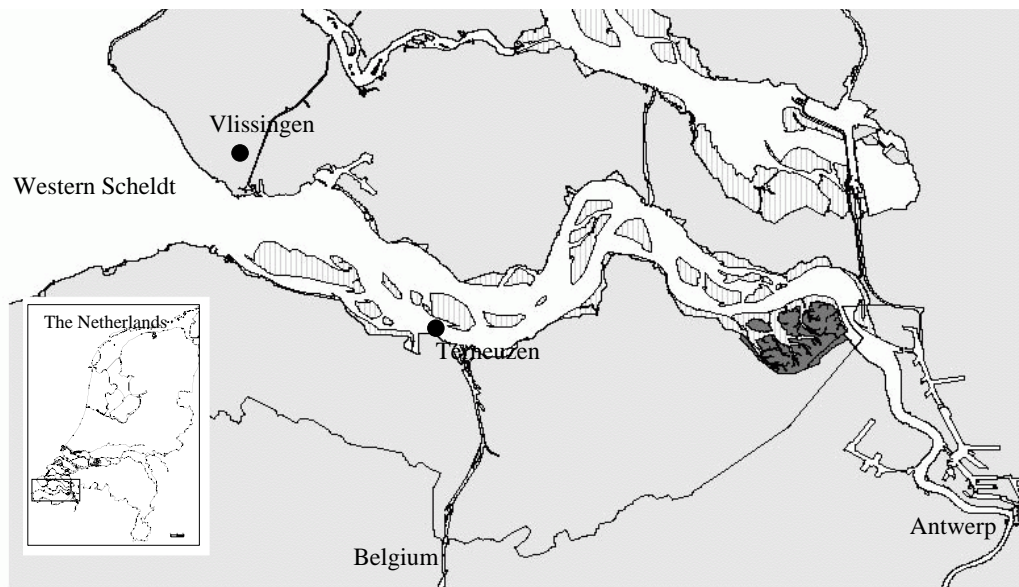


Figure 1: The marine salt and brackish part of the Western Scheldt estuary from Vlissingen to Antwerp.

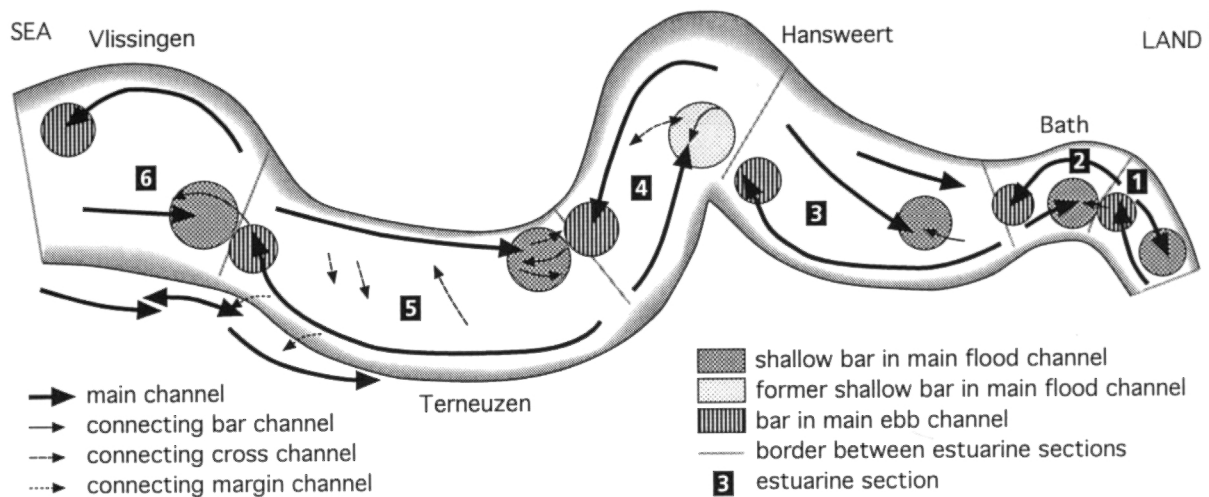


Figure 2: the six different estuarine sections in the Western Scheldt(from [6]).

Both for estuarine management and scientific purposes, fundamental knowledge about the behaviour of these bar–shoal systems is relevant.

Basically, three types of models can be used to study the morphological behaviour of estuaries and estuarine bars. The first type of models are the so–called semi–empirical models, see e.g. [17, 4]. In these models empirical relationships between various quantities are used. From a process–oriented perspective the evolution of bars has been successfully simulated by [20, 10]. These models are rather complex and have not been designed to gain fundamental understanding about the physical mechanisms controlling the channel–shoal dynamics. For the latter objective idealised models, which focus on isolated processes, are useful tools.

It has been demonstrated by [14] and [12] that bars in tidal embayments can form as inherent morphologic instabilities. [14] analyse a local model, which in general is designed to deal with phenomena that scale on a length scale which is small compared with both the tidal wave-length and embayment length. Thus, the dynamics is investigated in an infinitely long channel geometry. In this approach the water motion must be prescribed by specifying external pressure gradients which result from the dynamics on the global scale. In their study [14] use a three-dimensional model, based on the shallow water equations. They also a priori assume that the embayment width is the controlling length scale of the bed forms. Hence their model results apply to narrow, frictionally dominated tidal channels.

[12] on the other hand study a global model of a tidal embayment. This choice implies that they put emphasis on bottom patterns that occur on the length scale of the entire embayment. In this approach a semi-enclosed embayment is considered where the water motion is forced by a boundary condition at the entrance of the embayment. Their model is based on the depth-averaged shallow water equations and assumes that the ratio of the tidal excursion length and the embayment length is small. Results are presented for the case of a short embayment (with a length being much smaller than the tidal wave-length), in which sediment transport is dominated by diffusive processes and advective terms in the flow equations can be neglected. However, the model can be generalized in a straightforward sense, as is demonstrated in [13] (1D equilibrium dynamics in a long embayment) and [18] (2D nonlinear bed forms in a short embayment).

In this contribution the bed forms that are generated due to an inherent morphodynamic instability in a long embayment will be studied. It will be shown that both modes that scale with the embayment length and modes with a shorter wavelength are found. If the friction strength is increased, the modes with shorter lengthscales become much more unstable than the modes that scale with the embayment length. Furthermore, structures with shorter wavelengths are superposed on the modes scaling with the embayment length. It is proposed that the observed estuarine sections might be related to the spatial structure of the modes that scale with the embayment length.

2 Model description

In this contribution the water motion is described by the depth averaged shallow water equations (see [2]). These equations read

$$\zeta_t + [(H - h + \zeta)u]_x + [(H - h + \zeta)v]_y = 0, \quad (1a)$$

$$u_t + uu_x + vu_y + \frac{ru}{H - h + \zeta} = -g\zeta_x, \quad (1b)$$

$$v_t + uv_x + vv_y + \frac{rv}{H - h + \zeta} = -g\zeta_y, \quad (1c)$$

where the free surface is denoted by $z = \zeta$, the bottom of the estuary is found at $z = H - h$, and u and v denote the depth-averaged velocities in the longitudinal and lateral direction respectively. The bottom friction is modeled to depend linearly on the depth averaged velocity (see [7, 21]), the friction coefficient is denoted by r with dimensions ms^{-1} . Furthermore, Coriolis effects are neglected.

The dynamics of the suspended sediment is described by an advection-diffusion equation for the *volumetric* depth-integrated concentration C , which is the depth integrated sediment concentration (with dimension kg m^{-2}) divided by the sediment density [19]:

$$C_t + (uC - \mu C_x)_x + (vC - \mu C_y)_y = \alpha(u^2 + v^2) - \gamma C \quad (2)$$

The first term on the rhs models the sediment pick-up function, and the second term the tendency of sediment to settle due to gravity effects. The coefficients α ($\mathcal{O}(10^{-6} - 10^{-8}) \text{ s m}^{-1}$) and γ ($\mathcal{O}(10^{-3}) \text{ s}^{-1}$) depend on the sediment properties.

The evolution of the bottom follows from the conservation of sediment. Instead of solving the bed evolution on the short time scale, only the net effect during one tidal cycle is considered. Physically this means that the bed does not change appreciably during one tidal cycle but evolves on a much larger timescale. A good approximation is obtained by averaging the bottom evolution equation over one tidal cycle (denoted by $\langle . \rangle$) and reads

$$(1 - p)h_\tau = -\langle \alpha(u^2 + v^2) - \gamma C \rangle + \lambda \nabla^2 h \quad (3)$$

The first term on the right-hand side models the bed level changes due to erosion and deposition of

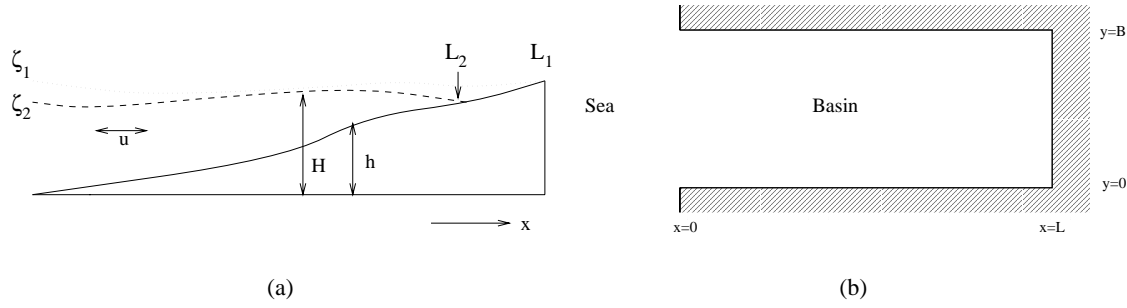


Figure 3: Top view (a) and side view (b) of the idealised embayment.

sediment, while the second term introduces the effects of bedslopes. This term is incorporated since suspended load is susceptible for the presence of local slopes (see [15, 8]). A system is considered to be in morphodynamic equilibrium when the divergences and convergences of the sediment flux, averaged over one tidal period, are zero. this implies that the bed does not change anymore.

The embayment consists of a semi-enclosed domain which is connected with the open sea (see figure 3). At the seaside the width-averaged free surface elevation is prescribed and the lateral velocity is forced to disappear. The bottom level is kept fixed at the entrance and becomes zero at the landward side of the estuary. At the sidewalls no water and sediment fluxes are allowed. Finally, at the landward side of the embayment the kinematic boundary condition is applied. For the concentration the sediment flux has to be zero and the bed level does not change in time. For a more extensive discussion of the model, see [13].

3 Linear stability analysis

For realistic values of the parameters the two-dimensional system of equations, as described in the previous section, allows for a morphodynamic equilibrium solution $\vec{\Psi}_{\text{eq}} = (u, v, \zeta, C, h)_{\text{eq}}$, which is spatially uniform in the lateral direction. The longitudinal structure and time-dependence of this equilibrium solution depends sensitively on the parameter values (see [13]). This equilibrium solution is in general not stable with respect to perturbations having a structure in the cross-channel direction. This means that such perturbations can grow due to a positive feedback between the water motion, the sediment transport and the erodible bed. The dynamics of the perturbations is analysed by substitution of

$$\vec{\Psi}(x, y, t, \tau) = \vec{\Psi}_{\text{eq}}(x, t) + \vec{\Psi}'(x, y, t, \tau)$$

in the full equations of motion. Here the variables are assumed to depend on two time variables: the fast coordinate t and the slow time coordinate $\tau = \delta t$, which measure the evolution of the system on the tidal timescale and morphologic timescale, respectively. The parameter $\delta \ll 1$ denotes the ratio of the tidal period and the morphologic timescale and is typically of order 10^{-3} .

Next it is assumed that the amplitude of the perturbations is small with respect to that of the equilibrium state. This allows for a linearization of the equations of motion. The linearized equations read

$$\begin{aligned} \zeta'_t + [(H - h_{\text{eq}} + \zeta_{\text{eq}})u']_x + [(H - h_{\text{eq}} + \zeta_{\text{eq}})v']_y \\ + [(-h' + \zeta')u_{\text{eq}}]_x + [-h' + \zeta']_y v_{\text{eq}} = 0, \end{aligned} \quad (4a)$$

$$u'_t + (u_{\text{eq}}u')_x + \frac{ru'}{H - h_{\text{eq}} + \zeta_{\text{eq}}} + \frac{ru_{\text{eq}}}{(H - h_{\text{eq}} + \zeta_{\text{eq}})^2}(h' - \zeta') = -g\zeta'_x, \quad (4b)$$

$$v'_t + u_{\text{eq}}v'_x + \frac{rv'}{H - h_{\text{eq}} + \zeta_{\text{eq}}} = -g\zeta'_y, \quad (4c)$$

$$C'_t + (u_{\text{eq}}C' + u'C_{\text{eq}} - \mu C'_x)_x + (v'C_{\text{eq}} - \mu C'_y)_y = 2\alpha u_{\text{eq}}u' - \gamma C', \quad (4d)$$

$$(1 - p)h'_t = -\langle 2\alpha u_{\text{eq}}u' - \gamma C' \rangle + \lambda \nabla^2 h'. \quad (4e)$$

The volumetric advective and diffusive sediment flux per unit of width, \vec{F}_a and \vec{F}_d respectively, are defined by

$$\vec{F}_a = (u_{\text{eq}}C' + u'C_{\text{eq}}, v'C_{\text{eq}}) \quad \text{and} \quad \vec{F}_d = (-\mu C'_x, -\mu C'_y).$$

The boundary conditions at the closed end of the embayment read

$$u'_x \text{ is finite,} \quad (5a)$$

$$\langle u'C_{\text{eq}} + u_{\text{eq}}C' - \mu C'_x \rangle = 0, \quad (5b)$$

$$\hat{C}(x, t, \mu) = \hat{C}(x, t, \mu = 0), \quad (5c)$$

$$h' = 0, \quad (5d)$$

where \hat{C} is the oscillatory part of the concentration. The first condition is the kinematic boundary condition; the second one states that no net sediment flux is allowed through the landward side of the embayment. The third condition states that no diffusive boundary layer develops in the time dependent part of the concentration and the last condition that the perturbed depth is zero and hence the length of the embayment is fixed. The boundary conditions at the seaward end read

$$\begin{cases} \zeta' = 0 & \text{if no lateral structure,} \\ v' = 0 & \text{if lateral structure,} \end{cases} \quad (6a)$$

$$\hat{C}(x, t, \mu) = \hat{C}(x, t, \mu = 0), \quad (6b)$$

$$\langle u'C_{\text{eq}} + u_{\text{eq}}C' - \mu C'_x \rangle_x = 0, \quad (6c)$$

$$h' = 0. \quad (6d)$$

The first condition states that, if the perturbations do not have a lateral structure, the sea level perturbation is zero. However, if a lateral structure is present, a perturbed sea level is allowed but the lateral velocities have to be zero. The perturbation of the sea level is then used to balance the forces exerted on the open boundary by both the advective and frictional contributions. The second condition states that no diffusive boundary layer develops at the seaside in the time dependent part of the concentration and the last two conditions state that both the convergence of sediment due to suspended load transport and slope effects must be zero. At the sidewalls the condition that both the water and sediment fluxes vanish, is imposed.

Careful examination of this system of equations shows that the perturbations are composed of the following eigenmodes:

$$\vec{\Psi}'(x, y, t, \tau) = \Re \left[e^{\omega\tau} \hat{\Psi}(x, y, t) \right]; \quad \hat{\Psi}(x, y, t) = \sum_{m,n} \vec{f}_m(x, t) \vec{g}_n(y). \quad (7)$$

Here \Re denotes the real part of the solution. The evolution of the perturbations on the slow morphodynamic timescale thus turns out to be exponential, with $\Re(\omega)$ denoting the growth rate and $-\Im(\omega)$ being the migration rate. The structure of the eigenfunction $g_n(y)$ in the lateral direction equals $\cos(l_n y)$, except for the second component which reads $\sin(l_n y)$. Here $l_n = n\pi/B$ where $n = 0, 1, 2, \dots$ is the cross-channel mode number. Furthermore, on the short timescale the flow and concentration consists of a superposition of tidal harmonics (M_2, M_4, \dots) and a residual component. Of course the bed perturbation h' only has a residual component on the tidal timescale, see remarks above (3). Using this information, the system of equations and boundary conditions yields an *eigenvalue* problem for the eigenfunction structure in the longitudinal direction, $f_m(x, t)$, and grow rate ω .

This eigenvalue problem is solved by first making an expansion up to first order with respect to the small parameters $\epsilon \equiv U/\sigma L$. Hence the following expansions are made:

$$\Phi = \Phi_0 + \epsilon \Phi_1 \dots, \quad (8)$$

with

$$\Phi_0 = \Phi^s \sin(t) + \Phi^c \cos(t), \quad (9a)$$

$$\Phi_1 = \langle \Phi \rangle + \Phi^{2s} \sin(2t) + \Phi^{2c} \cos(2t) \quad (9b)$$

where Φ is any of the variables ζ' , u' , and v' . For \hat{C}' a similar kind of expansion is made. The component Φ_0 describes the main tidal constituent, and $\langle \Phi \rangle$ describes the mean contributions generated by nonlinear interactions. By definition $\langle \hat{C}' \rangle = 0$. Furthermore, Φ^{2c} and Φ^{2s} are the internally generated M_4 overtide. By this expansion an eigenvalue problem is obtained, which can be solved using standard numerical techniques.

4 Results

In this section an embayment with characteristics similar to those of the marine part of the Western Scheldt is studied. The length of the embayment is 60 km, the depth at the entrance is 10 m, at the landward side the water depth vanishes. The system is only forced by an externally prescribed M_2 tide with an amplitude of 1.5 m, higher harmonics in the external forcing are neglected. The width of the rectangular embayment is 5 km. Both for the global equilibrium and the bedforms that start to grow as linear instabilities on this equilibrium, the parameterisation of the bottom friction and the magnitude of the diffusion constant μ are very important. In these experiments, $r = 0.0004 \text{ m s}^{-1}$ and $\mu = 25 \text{ m}^2 \text{ s}^{-1}$. Note that the value for r has been taken rather small. This will be discussed in more detail in section 5. In this experiment the ratio δ of the tidal time scale and the morphologic time scale is 0.007. The growth rates are made dimensionless by scaling them with $\delta\sigma$, where σ is the tidal frequency.

In figure 4 the morphodynamic equilibrium bed profile and M_2 vertical amplitude are plotted as function of the position in the embayment. These equilibrium profiles are independent of the lateral direction. The increase of the amplitude of the M_2 horizontal level towards the entrance of the embayment (see figure 4(b)) indicates that the system is resonant.

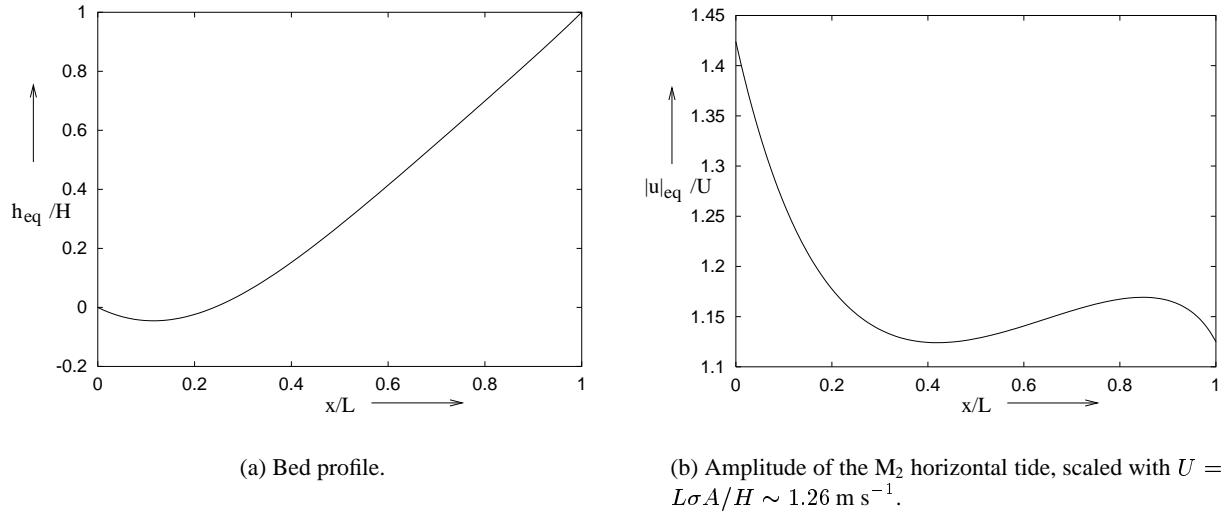


Figure 4: Morphodynamic equilibrium for a rectangular embayment with a length of 60 km. The system is forced by a M_2 tide with an amplitude of 1.5 m.

This equilibrium is not stable with respect to perturbations with a structure in the lateral direction. In this contribution we will study the instabilities with small lateral mode numbers ($n \leq 4$). This is motivated by the fact that for these lateral mode numbers the two different types of modes, i.e., the modes that scale with the embayment width and the modes scaling with the length of the embayment, can be most easily distinguished.

For the lateral mode number $n = 0$ only modes scaling with the embayment length are found. In figure 5 the bottom profiles of the first three eigenmodes are shown. All the eigenmodes are linearly damped. This means that, if a bottom perturbation without lateral structure is superposed on the equilibrium bottom profile, the amplitude of this perturbation decreases and the system evolves towards the unperturbed equilibrium.

If the mode number is increased, the equilibrium bed profile becomes unstable, i.e., the amplitude of some of the bed perturbations starts to increase. The most unstable modes are those that have a lengthscale much shorter than the embayment length. In figure 6 the real and imaginary part of the

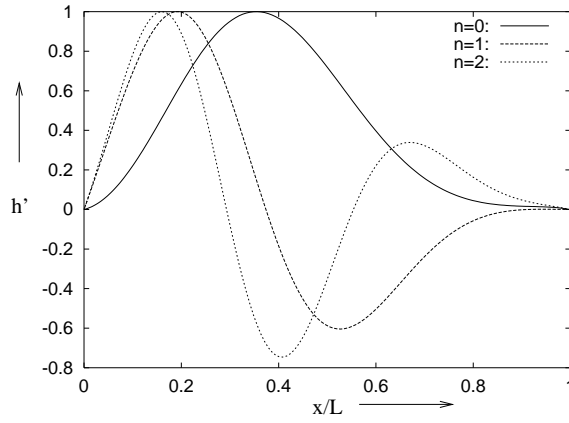


Figure 5: The bed profiles of the three most unstable eigenfunctions with no lateral structure ($n = 0$). Here the maximum amplitude of the bed perturbation is scaled to one.

most unstable bed profile is plotted. The growth rate $\Re(\omega)$ equals 0.057 and its frequency is given by $-\Im(\omega) = 0.011$. Remember that physically relevant quantities are obtained by taking the real part of $h'(x)e^{\omega\tau}$ (see expression (7)). In figure 7 the advective and diffusive fluxes that result in the growth of the

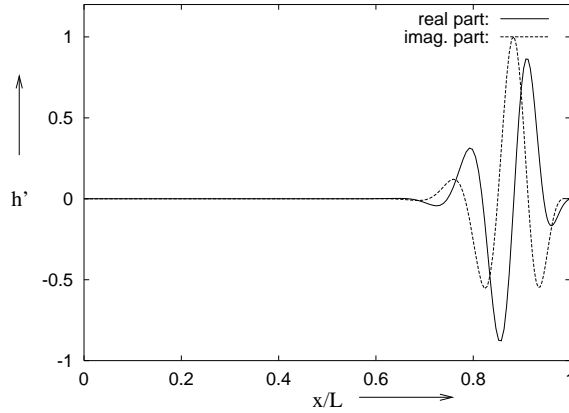
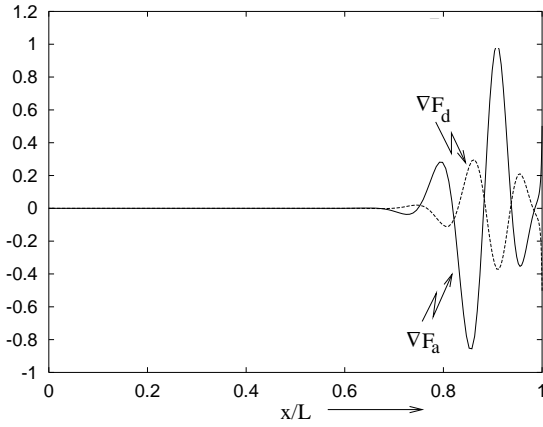


Figure 6: The real and imaginary part of the bottom structure of the first most unstable eigenfunction in the longitudinal direction with lateral mode number $n = 1$). Here the maximum amplitude of the bed perturbation is scaled to one.

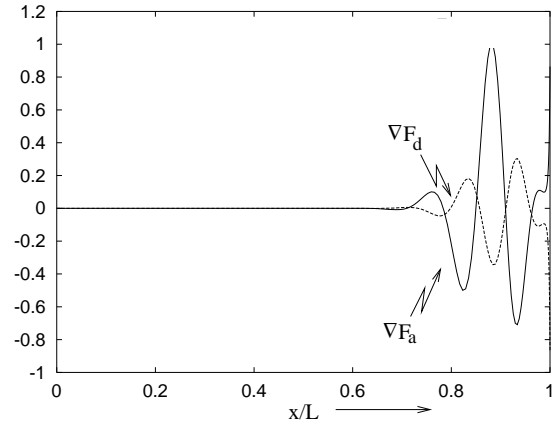
eigenfunction are shown. These figures show that the net convergences and divergences of the *advective* fluxes result in the growth of the perturbations, whereas the *diffusive* fluxes suppress the growth of these local modes. The physical mechanism resulting in the growth of the local modes has been extensively discussed in [11].

Apart from bed perturbations that have lengthscales much shorter than the embayment length, bottom structures that scale with the length of the embayment are found as well. The most unstable global mode with $n = 1$ is the eleventh mode, i.e., ten modes with length scales much shorter than the embayment length are more unstable than this global mode. Its structure is shown in figure 8(a). For the parameter values used here, this mode is still linearly damped. However, by increasing friction it can become unstable as well. In figure 8(b) the fluxes associated with this global mode are plotted. From this figure it is clear that *diffusive* fluxes are dominating in most of the embayment. The diffusive fluxes result in a perturbation that scales with the length of the embayment. The instability mechanism is already described in [12]. The advective fluxes modify the structure of the global mode with structures that have shorter wavelengths. In figure 8(a) the dotted line shows the global bed perturbation without the local oscillations.

This picture is still valid for $n > 1$. The modes generated by divergences and convergences of advective fluxes, are the most unstable perturbations. The growth rates of the most unstable local structure in the longitudinal direction is increasing with lateral mode number. Modes that scale with the embayment

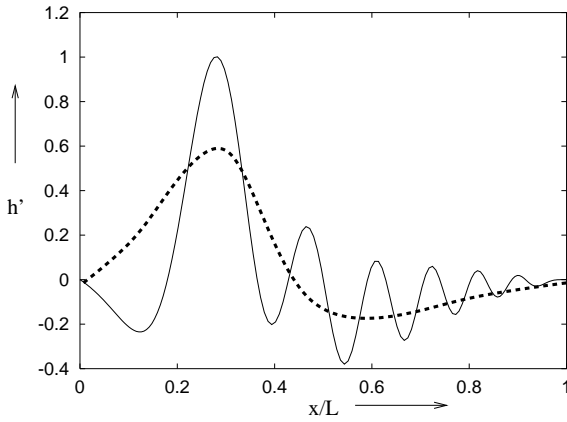


(a) Real part of the fluxes.

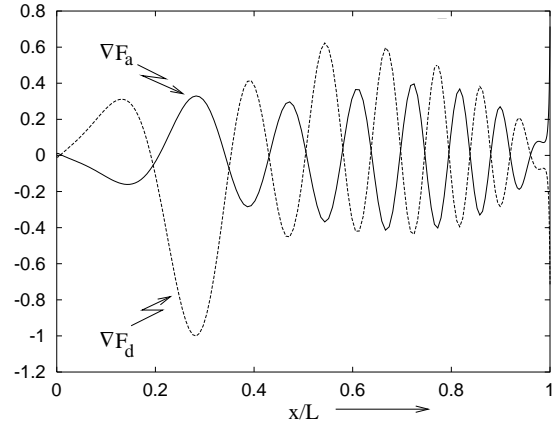


(b) Imaginary part of the fluxes.

Figure 7: The divergences and convergences of the advective and diffusive sediment fluxes for the most unstable eigenfunction with $n = 1$. The divergences of the fluxes are scaled with the maximum divergence of the (advective) flux in the domain.



(a) Most unstable global bed profile for $n = 1$.



(b) Divergence of the sediment fluxes associated with the most unstable mode scaling with the embayment length.

Figure 8: The bottom structure and associated divergences and convergences of the advective and diffusive sediment fluxes for the most unstable global mode with $n = 1$. The divergences of the fluxes are scaled with the maximum divergence of the (diffusive) flux in the domain. The dotted line shows the global bed perturbation (without the local structures).

length are present as well, generated by divergences and convergences of diffusive fluxes. The fact that the small-scale modes are much more unstable than the global modes is to be expected since in long embayments advective processes ($\sim \sigma A^2 H^{-2}$) are much more efficient than diffusive ones ($\sim \mu/L^2$). The modes scaling with the embayment length are modified by structures with shorter wavelengths. In figure 9 the most unstable global modes for $n = 2, 3$ and 4 are plotted.

The most unstable global mode with longitudinal mode number m and lateral mode number n can be interpreted as the initial formation of structures resembling estuarine sections. Here the longitudinal number of zeros is a measure for the number of estuarine sections, while the lateral mode numbers characterise the number of channels. Consider for example the most unstable global mode with $n = 4$. The bed profile associated with this eigenfunction has 4 estuarine sections, in which the lateral structure consists alternatingly of two channels/three shoals and three channels/two shoals (see figure 9(c)). It

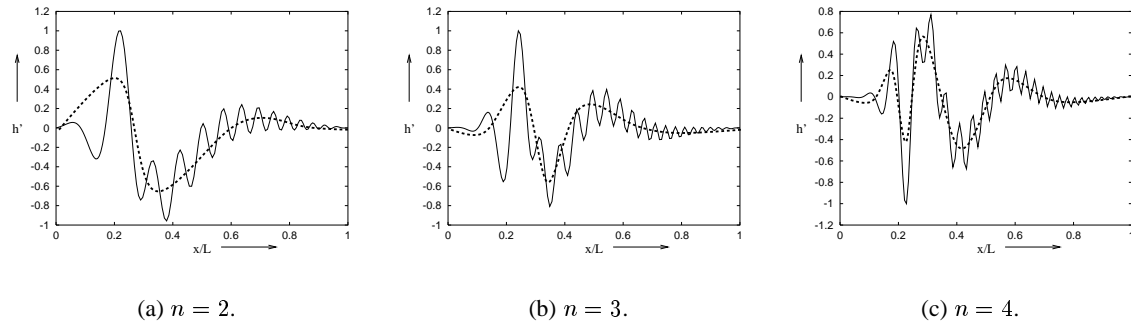


Figure 9: The bottom structures of the most unstable global modes with $n = 2, 3$ and 4 . Note that, as n increases, the local structures have smaller wavelengths. The dotted line shows the global bed perturbation (without the local structures). Here the maximum amplitude of the bed perturbation is scaled to one.

is very important to know which global mode is most unstable, since this determines the exact number of sections and channels. This turns out to be very sensitive for the friction value, geometry and tidal characteristics and is currently being studied.

5 Discussion and conclusions

A global model is discussed that describes the initial formation of bed forms in tidal embayments. In this model, two types of instabilities are encountered: modes that scale with the length of the embayment and modes that are characterised by shorter wavelengths. The physical processes involved depend on tidal and geometrical characteristics of the underlying equilibrium. For the global modes the spatial structure of the underlying morphodynamic equilibrium is crucial as well. The most unstable global mode is characterised by a longitudinal mode number m and a lateral mode number n . It is proposed that the number of estuarine sections can be related to m of the most unstable global mode, while n counts the number of channels in the lateral direction. From the experiments it follows that both m and n of the most unstable global mode are highly dependent on the friction parameter. It is shown that on the global modes structures that have shorter lengthscales are superimposed. For realistic values of the friction parameter it is very difficult to make a clear distinction between global and local modes. This is one of the points of current research, since this question has to be solved in order to develop a nonlinear model that describes the long-time behaviour of the estuarine sections.

Since the fine-structured bedforms of the global model and the bars in the local models must be the same features in the appropriate limit, the results from these two approaches should qualitatively agree in the appropriate limits. This is not straightforward, because the local model of [14] and the nonlinear global model of [13] use different formulations and assumptions. This motivated the set up of an intermediate model, in which both the embayment width and the tidal excursion length, were retained as relevant length scales. Hence this model can deal with phenomena that scale on a length scale which is small compared with both the tidal wave-length and embayment length, but not necessarily small compared with the tidal excursion length. This intermediate model serves as a link between the two models. It has already been shown that in the limit of a narrow channel (see [11]), the bedforms found by [14] are recovered. In a forthcoming paper the connection with the local modes found in the global model will be made.

Acknowledgement

This research was supported by the National Institute for Coastal and Marine Management at The Hague, The Netherlands.

References

- [1] J. Cleveringa and A. P. Oost. The fractal geometry of tidal channel systems in the dutch wadden sea. *Geologie en Mijnbouw*, 78:21–30, 1999. Special Issue on Prediction in Geology.
- [2] G. T. Csanady. *Circulation in the coastal ocean*. Reidel, Dordrecht, 1982.
- [3] R. W. Dalrymple and R. M. Rhodes. Estuarine dunes and bars. In G. M. E. Perillo, editor, *Geomorphology and Sedimentology of Estuaries*, volume 53 of *Development in Sedimentology*, pages 359–422. Elsevier, New York, 1995.
- [4] G. Di Silvio. Modelling the morphological evolution of tidal lagoons and their equilibrium configurations. In *Proc. XIIIrd IAHR Congress*, pages C169–C175. IAHR, 1989.
- [5] J. Ehlers. *The Morphodynamics of the Wadden Sea*. Balkema, Rotterdam, 1988.
- [6] M. C. J. L. Jeuken. On the morphologic behaviour of tidal channels in the westerschelde estuary. volume 279 of *Netherlands geographical studies*. KNAG, 2000.
- [7] H. A. Lorentz. Het in rekening brengen van den weerstand bij schommelende vloeistofbewegingen. *De Ingenieur*, page 695, 1922.
- [8] G. Parker. Self-formed straight rivers with equilibrium banks and mobile bed. part 1. the sand-silt river. *J. Fluid Mech.*, 89:109–125, 1978.
- [9] G. M. E. Perillo, editor. *Geomorphology and sedimentology of estuaries*, Developments in sedimentology 53, New York, 1995. Elsevier.
- [10] R. Ranasinghe, C. Pattiaratchi, and G. Masselink. A morphodynamic model to simulate the seasonal closure of tidal inlets. *Coastal Eng.*, 37:1–36, 1999.
- [11] G. P. Schramkowski, H. M. Schuttelaars, and H. E. De Swart. In C. T. Friedrichs and A. Valle-Levinson, editors, *Physics of Estuaries and Coastal Seas*. PECS 2000, submitted to JCR.
- [12] H. M. Schuttelaars and H. E. De Swart. Initial formation of channels and shoals in a short tidal embayment. *J. Fluid Mech.*, 386:15–42, 1999.
- [13] H. M. Schuttelaars and H. E. De Swart. Multiple morphodynamic equilibria in tidal embayments. *J. Geo. Res.*, 105:24105–24118, 2000.
- [14] G. Seminara and M. Tubino. On the formation of estuarine free bars. In J. Dronkers and M.B.A.M. Scheffers, editors, *Physics of Estuaries and Coastal Seas*, pages 345–353, Rotterdam, 1998. PECS 96, Balkema.
- [15] A. M. Talmon, M. C. L. M. van Mierlo, and N. Struiksmā. Laboratory measurements of the direction of sediment transport on transverse alluvial-bed slopes. *J. Hydr. Res.*, 33:495–517, 1995.
- [16] J.H. Van den Berg, M.C.J.L. Jeuken, and A.J.F. van der Spek. Hydraulic processes affecting the morphology and evolution of Westerschelde estuary. In K.F. Nordstrom and C.T. Roman, editors, *Estuarine shores: Evolution, Environments and Human Alterations*, pages 157–184, Chichester, 1997. John Wiley and Sons Ltd.
- [17] A. R. Van Dongeren and H. J. de Vriend. A model of morphological behaviour of tidal basins. *Coastal Eng.*, 22:287–310, 1994.
- [18] S. M. Van Leeuwen and H. E. De Swart. Title. *J. Fluid Mech.*, in preparation.
- [19] L. C. Van Rijn. *Principles of sediment transport in rivers, estuaries and coastal seas*. Aqua Publ., Amsterdam, 1993.
- [20] Z.B. Wang, T. Louters, and H.J. De Vriend. Morphodynamic modelling for a tidal inlet in the Wadden Sea. *Mar. Geol.*, 126:289–300, 1995.
- [21] J. T. F. Zimmerman. On the Lorentz linearization of a quadratically damped forced oscillator. *Phys. Lett.*, 89A:123–124, 1982.